Two DO-CCII Based Lossless Floating Capacitance Multipliers

Tolga Yucehan [1] iD

[1]*Afyon Kocatepe University, Dazkiri Vocational School, Afyonkarahisar, TURKEY*

Abstract

In this paper, two new lossless floating capacitance multipliers (FCMs) are designed. These FCMs consist of two dual-output second-generation current conveyors (DO-CCIIs). In the designed FCMs, two resistors and a capacitor are used. The resistors of the proposed FCMs are grounded. Nevertheless, the capacitors of the FCMs are floating. The proposed circuits can be electronically adjusted if current controlled DO-CCIIs are employed instead of the DO-CCIIs in the proposed lossless FCMs. Furthermore, passive element matching conditions do not necessary for the proposed circuits. The proposed FCMs are tested in the second-order passive filter. The SPICE program is carried out for all the simulations while utilizing the parameters of the 0.18 µm CMOS technology.

Key Words

"Lossless, DO-CCII, floating capacitance multipliers"

*Corresponding Author: tyucehan@aku.edu.tr

1. Introduction

In analog circuits, such as oscillators and active filter circuits, a capacitor has a crucial role as a passive component. As mentioned in (Amico et al., 1997), large-valued capacitors are unsuitable for integrated circuit (ICs) technologies due to their large area requirements. It means that as the value of the capacitor increases, the area of the ICs also increases. The capacitance multiplier circuits are utilized instead of large-sized capacitors in IC technology. In the literature, various types of active block buildings (ABBs) are used in analog circuit designs (Kuntman & Uygur, 2012). Current-mode (CM) active devices offer several potential benefits over voltage-mode (VM) active devices like operational amplifiers (Giuseppe & Guerrini, 2004; Senani et al., 2015; Toumazou et al., 1993; Wilson, 1990, 1992). Among them, one of the most commonly used ABB is the second-generation current conveyor (CCII), especially in low-power applications and CM signal processing (Ferri & Guerrini, 2001; Yuce, 2017). However, some CCII-based floating capacitance multiplier (FCM) circuits mentioned in the literature have some disadvantages, which are listed below:

The circuits mentioned in (Abuelma'Atti & Tasadduq, 1999; Al-Absi & Al-Khulaifi, 2019; Jaikla & Siripruchyanun, 2007; Pal, 1981; Saad & Soliman, 2010; Senani, 1982; Siripruchyanun et al., 2007; Yuce, Minaei, et al., 2006; Yuce, 2006a, 2006b; Yuce, Cicekoglu, et al., 2006; Yucehan & Yuce, 2022) have been implemented using more than two ABBs. In the FCM circuits introduced in (Jaikla & Siripruchyanun, 2007; Yuce, 2006a, 2006b), more than two resistors are utilized. The ABBs employed in some of the proposed circuits are not similar (Al-Absi & Al-Khulaifi, 2019; Jaikla & Siripruchyanun, 2007; Saad & Soliman, 2010; Sagbas et al., 2009; Siripruchyanun et al., 2007). Additionally, the FCM has a passive element matching issue in (Yuce, 2006a), while the FCM presented in (Abuelma'Atti & Tasadduq, 1999) is lossy. Furthermore, the FCM circuits described in (Abuelma'Atti & Tasadduq, 1999; Jaikla & Siripruchyanun, 2007; Minaei et al., 2006; Petchakit & Petchakit, 2005; Siripruchyanun et al., 2007; Yuce, 2006b; Yuce, Minaei, et al., 2006) are included BJTs in the internal structure of the ABBs. In this case, the proposed circuits are sensitive to temperature variations. A comparison of these CCII-based FCMs from the literature with the proposed circuits is presented in **Table 1**.

This study proposes two new lossless FCM circuits. Two dual-output CCIIs (DO-CCIIs) are utilized in both proposed FCMs. The FCMs are designed with a minimum number of passive elements, consisting of one capacitor and two resistors. The resistors are grounded; nevertheless, the capacitors in the proposed FCMs are floating. The circuits can be electronically adjustable if current-controlled DO-CCIIs (DO-CCCIIs) are used instead of the ABBs. The ideal and non-ideal analyses of the FCMs are performed. Also, the FCMs are examined in a second-order passive filter as an application. All the simulations are performed using the SPICE program.

The rest of the study is planned as follows: In the second section, the DO-CCII is introduced, while the proposed circuits and their theoretical analyses are presented in Section 3. The simulation results of the proposed FCMs are introduced in Section 4. The application circuit and its simulations are given in the fifth section. Finally, the conclusion is discussed in Section 6.

Table 1. The Comparison table for the FCMs in the literature and the proposed ones.

References (Figure)	Lossless	# of Resistors G / F	Using Capacitor	Technology	# of ABBs	Using Similar ABBs	Supply Voltages (V)	Total Power Consumptions (W)	Matching Conditions	Operating Frequency Range (Decade)
(Abuelma'Atti & Tasadduq, 1999) (4)	No	0 / 0	G	BJT	DO-CCCII, 3 CCCII+	Yes	± 2.5	-	No	-
(Al-Absi & Al-Khulaifi, 2019) (1)	Yes	0 / 0	F	0.18μm	CCII+, 4 OTA	No	± 0.75	2.03 μ	No	7
(Jaikla & Siripruchyanun, 2007) (3)	Yes	4 / 0	G	BJT	DVCC, DO-CCII, CCII+, CCII-	No	± 1.5	-	No	3.48
(Minaei et al., 2006) (1)	Yes	1 / 1	G	BJT	2 DO-CCII	Yes	± 2.5	-	No	-
(Mohan, 2005) (1.a)	Yes	1 / 1	G	-	2 DO-CCII	Yes	-	-	No	-
(Pal, 1981) (2)	Yes	1 / 1	G	-	2 CCII+, 2 CCII-	Yes	-	-	No	-
(Petchakit & Petchakit, 2005) (3)	Yes	1 / 1	G	BJT	2 DO-CCII	Yes	± 2.5	-	No	-
(Saad & Soliman, 2010) (14)	Yes	1 / 1	G	0.25 μm	DVCC, 2 CCII+	No	± 1.5	-	No	2
(Sagbas et al., 2009) (1)	Yes	1 / 0	G	0.35 μm	DO-CCII, OTA	No	± 1.5	1m	No	4.75
(Senani, 1982) (1)	Yes	1 / 1	G	-	4 CCII+	Yes	-	-	No	-
(Siripruchyanun et al., 2007) (3)	Yes	2 / 0	G	BJT	DVCC, DO-CCCII, CCCII+, CCCII-	No	± 1.5	-	No	3.48
(Yuce, 2006a) (1)	Yes	3 / 0	G	0.35 μm	DO-CCII, CCII+, CCII-	Yes	± 1.5	-	Yes	4
(Yuce, 2006b) (1)	Yes	3 / 0	G	BJT	DO-CCCII, 3 CCCII+	Yes	± 2.5	-	No	-
(Yuce, 2006b) (2)	Yes	3 / 0	G	BJT	2 DO-CCCII, CCCII+	Yes	± 2.5	-	No	-
(Yuce, Cicekoglu, et al., 2006) (1)	Yes	1 / 1	G	0.35 μm	DO-CCII, CCII+, CCII-	Yes	± 1.5	-	No	1.52
(Yuce, Minaei, et al., 2006) (4)	Yes	0 / 0	G	BJT	DO-CCCII, 3 CCCII+	Yes	± 2.5	-	No	-
(Yucehan & Yuce, 2022) (5)	Yes	1 / 1	G	0.18 μm	2 DO-CCII, CCII-	Yes	± 1.25	1.26 m	No	5
First Proposed FCM	**Yes**	**2 / 0**	**F**	**0.18 μm**	**2 DO-CCII**	**Yes**	**± 1.25**	**1.16 m**	**No**	**6.12**
Second Proposed FCM	**Yes**	**2 / 0**	**F**	**0.18 μm**	**2 DO-CCII**	**Yes**	**± 1.25**	**1.16 m**	**No**	**6.12**

G: Grounded   F: Floating   -: Not available

2. The Presentation of the DO-CCII

The symbolic demonstration of the DO-CCII is given in **Figure 1**. The mathematical equation of the terminals of the DO-CCII, with the non-ideal gains, is defined in equation (1) as a matrix form. In equation (1), β, α, and γ are terms that specify non-ideal gains in which β is voltage gain, while α and γ are current gains. The internal structure of the DO-CCII based on CMOS transistors is obtained from (Hassanein et al., 2005), which is demonstrated in **Figure 2**.
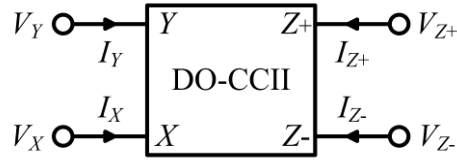
Figure 1. The symbolic demonstration of the DO-CCII

$$\begin{bmatrix} I_Y \\ V_X \\ I_{Z+} \\ I_{Z-} \end{bmatrix} = \begin{bmatrix} 0 & 0 \\ \beta & 0 \\ 0 & \alpha \\ 0 & -\gamma \end{bmatrix} \begin{bmatrix} V_Y \\ I_X \end{bmatrix} \tag{1}$$
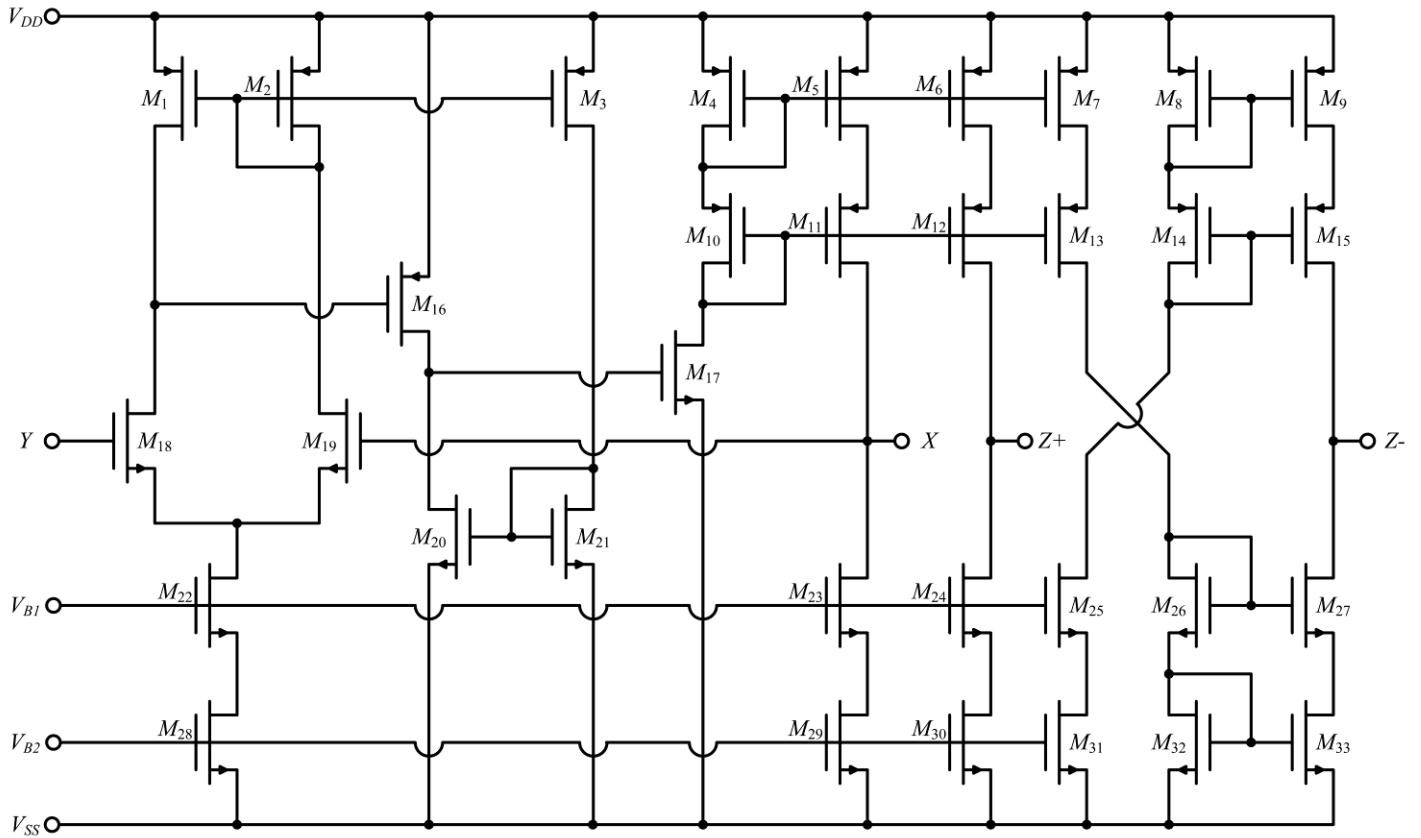
Figure 2. The internal structure of the DO-CCII based on CMOS transistors derived from (Hassanein et al., 2005)

3. Proposed Circuits

The proposed lossless FCMs are demonstrated in **Figure 3** and **Figure 4**, respectively. Two DO-CCII, a capacitor, and two resistors are used in each designed FCM. Also, the equivalent representation of the designed FCMs is given in **Figure 5**.
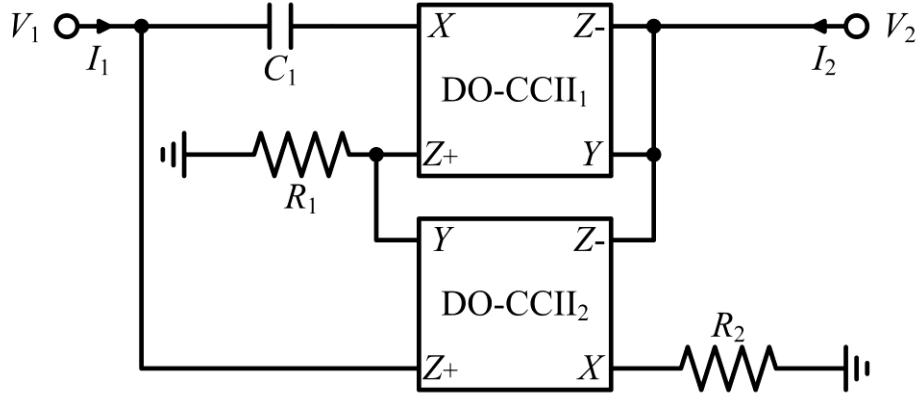
Figure 3. The first proposed FCM
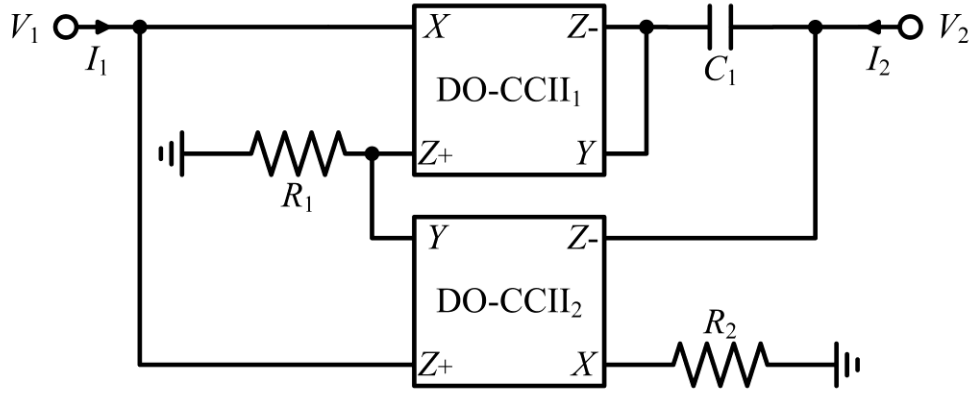
Figure 4. The second proposed FCM
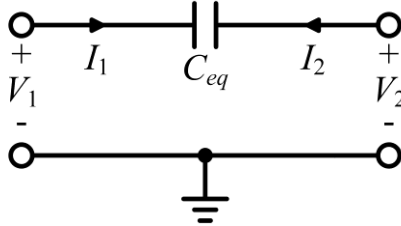
Figure 5. The equivalent representation of the designed FCMs

3.1. Theoretical Analyses of The First Proposed FCM

The first proposed FCM, which is shown in **Figure 3**, is ideally calculated as in equation (2).

$$\begin{bmatrix} I_1 \\ I_2 \end{bmatrix} = sC_1\left(1+\frac{R_1}{R_2}\right)\begin{bmatrix} 1 & -1 \\ -1 & 1 \end{bmatrix}\begin{bmatrix} V_1 \\ V_2 \end{bmatrix} = sC_{eq}\begin{bmatrix} 1 & -1 \\ -1 & 1 \end{bmatrix}\begin{bmatrix} V_1 \\ V_2 \end{bmatrix} \tag{2}$$

Here, C_{eq} is an equivalent capacitance, while K is a multiplying factor, and they are respectively equal to $C_1(1+R_1/R_2) = C_1K$ and $1+R_1/R_2$. If the non-ideal gains of the DO-CCII are included, the matrix equation is evaluated as

$$\begin{bmatrix} I_1 \\ I_2 \end{bmatrix} = \frac{sC_1}{R_2}\begin{bmatrix} \alpha_1\alpha_2\beta_2R_1 + R_2 & -\beta_1\left(\alpha_1\alpha_2\beta_2R_1 + R_2\right) \\ -\left(\alpha_1\beta_2\gamma_2R_1 + \gamma_1R_2\right) & \beta_1\left(\alpha_1\beta_2\gamma_2R_1 + \gamma_1R_2\right) \end{bmatrix}\begin{bmatrix} V_1 \\ V_2 \end{bmatrix} \tag{3}$$

If the parasitic impedances of the DO-CCII are included, while the DO-CCII is considered ideal, the following matrix equation is calculated as

4

$$\begin{bmatrix} I_1 \\ I_2 \end{bmatrix} = \frac{1}{b}\begin{bmatrix} 1+a+b\left(C_{Z+}//R_{Z+}\right) & -(1+a) \\ -(1+a) & 1+a+b\left(C_Y//2C_{Z-}//2R_{Z-}\right) \end{bmatrix}\begin{bmatrix} V_1 \\ V_2 \end{bmatrix} \tag{4}$$

where the terms, *a* and *b*, are defined as

$$a = \left(C_Y//C_{Z+}//R_{Z+}//R_1\right)\left(R_X + R_2\right) \tag{5a}$$

$$b = a\left(R_X + \frac{1}{sC_1}\right) \tag{5b}$$

3.2. Theoretical Analyses of The Second Proposed FCM

The second proposed FCM, which is represented in **Figure 4**, is ideally evaluated as in equation (2). When considering the non-ideal gains of the DO-CCII, the equation is calculated as in equation (6).

$$\begin{bmatrix} I_1 \\ I_2 \end{bmatrix} = \frac{sC_1}{\gamma_1 R_2}\begin{bmatrix} \beta_1\left(\alpha_1\alpha_2\beta_2 R_1 + R_2\right) & -\left(\alpha_1\alpha_2\beta_2 R_1 + R_2\right) \\ -\beta_1\left(\alpha_1\beta_2\gamma_2 R_1 + \gamma_1 R_2\right) & \alpha_1\beta_2\gamma_2 R_1 + \gamma_1 R_2 \end{bmatrix}\begin{bmatrix} V_1 \\ V_2 \end{bmatrix} \tag{6}$$

If the parasitic impedances of the DO-CCII are considered, while the non-ideal gains of the DO-CCII are chosen as unity, the following matrix equation is calculated as

$$\begin{bmatrix} I_1 \\ I_2 \end{bmatrix} = \frac{1}{ad}\begin{bmatrix} (1+a)\left[\left(C_Y//C_{Z-}//R_{Z-}\right)+sC_1\right]+ad\left(C_{Z+}//R_{Z+}\right) & -(1+a)sC_1 \\ -(1+a)sC_1-\left(C_Y//C_{Z-}//R_{Z-}\right) & ad\left(C_{Z-}//R_{Z-}\right)+(1+ac)sC_1 \end{bmatrix}\begin{bmatrix} V_1 \\ V_2 \end{bmatrix} \tag{7}$$

where the term, *a*, is given in equation (5a), while terms, *c* and *d*, are shown in equations (8a) and (8b), respectively.

$$c = 1 + R_X\left(C_Y//C_{Z-}//R_{Z-}\right) \tag{8a}$$

$$d = c + sC_1 R_X \tag{8b}$$

4. Simulations of The Proposed FCMs

The sizes of the MOS transistors in the internal structure are given in **Table 2**. The supply voltages, V_{DD} and V_{SS}, are respectively selected as +1.25 V and –1.25 V, while bias voltages, V_{B1} and V_{B2}, are chosen as –0.25 V and –0.62 V. The non-ideal gains and parasitic impedance values of the MOS transistor-based DO-CCII in **Figure 2** are obtained as indicated in **Table 3**. Additionally, the 0.18 µm CMOS technology parameters specified in (Minaei & Yuce, 2010) are utilized for the MOS transistors in **Figure 2**. The SPICE program is used for all the simulations.

Table 2. Sizes of the MOS transistors

	MOS Transistors	W (µm)	L (µm)
PMOS	M_1-M_{16}	18	
NMOS	M_{18}, M_{19}, M_{22}, M_{28}	6	0.5
	M_{17}, M_{20}, M_{21}, M_{23}-M_{27}, M_{29}-M_{33}	5	

Table 3. Several achievement parameters of the DO-CCII

Non-ideal Gain Parameter Values			Values of The Parasitic Impedances		
$\alpha_0 = 1.0000$	$\beta_0 = 1.0000$	$\gamma_0 = 0.9997$	$R_X = 0.5162\ \Omega$	$R_{Z+} = 20.407\ M\Omega$	$R_{Z-} = 22.512\ M\Omega$
$f_{\alpha 0} = 405$ MHz	$f_{\beta 0} = 510$ MHz	$f_{\gamma 0} = 340$ MHz	$C_Y = 4.79$ fF	$C_{Z+} = 16.64$ fF	$C_{Z-} = 33.29$ fF

4.1. Simulation Results of The First Proposed FCM

In many simulations for the first proposed FCM, which is shown in **Figure 3**, C_1 is selected as 50 pF, and R_1 is chosen as 10 kΩ while R_2 is 1 kΩ. As a result, K is calculated as 11 while C_{eq} is 0.55 nF. The first proposed FCM is consumed 1.16mW of power. AC frequency-domain results of the first proposed FCM are represented in **Figure 6** comparatively with the ideal results. Also, Monte Carlo (MC) analyses are performed, while the uniform deviations of all passive elements are selected as 10%. MC analyses are made for 150 samples. MC results of the first proposed FCM are demonstrated in **Figure 7**. The temperature analysis results are shown in **Figure 8**, in which the temperature is changed from –40ºC to 120ºC. In addition to these analyses, the time-domain analysis of the first proposed FCM is fulfilled. The sinusoidal input currents, which have 20 µA peak-to-peak magnitude and 100 kHz frequency, are applied separately in the designed FCM and equivalent FCM circuits. The input current and output voltages are indicated in **Figure 9**. AC responses of the first proposed FCM with different K values are given in **Figure 10**. In this analysis, C_1 and R_2 are respectively chosen as 50 pF and 1 kΩ. Furthermore, R_1 is separately selected as 1 kΩ, 99 kΩ, and 999 kΩ. As a result, C_{eq} is obtained as 100 pF, 0.5 nF, and 5 nF, while K is evaluated as 2, 100, and 1000, respectively.
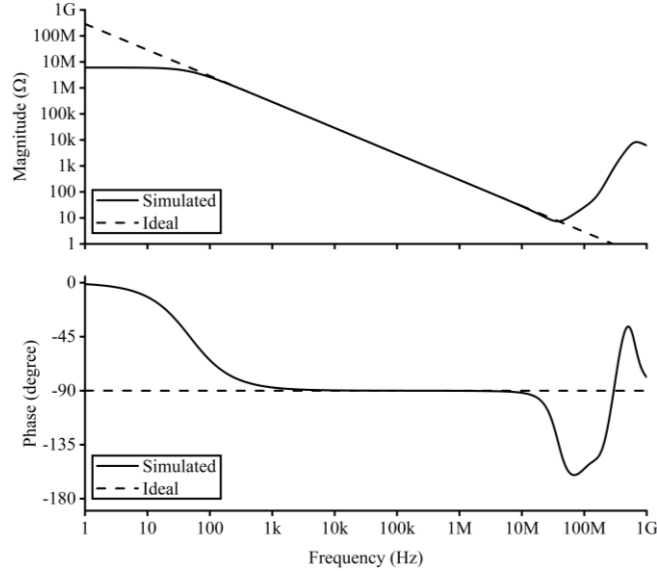
Figure 6. AC analysis outcomes of the first proposed FCM
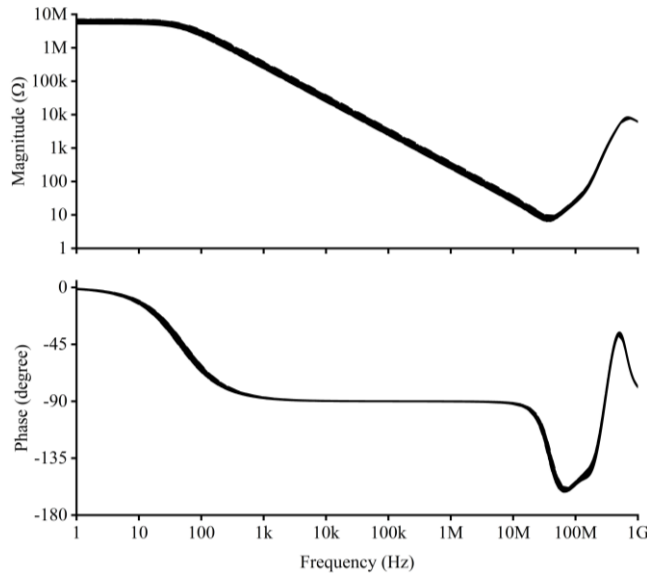
Figure 7. MC analysis outcomes of the first proposed FCM

6
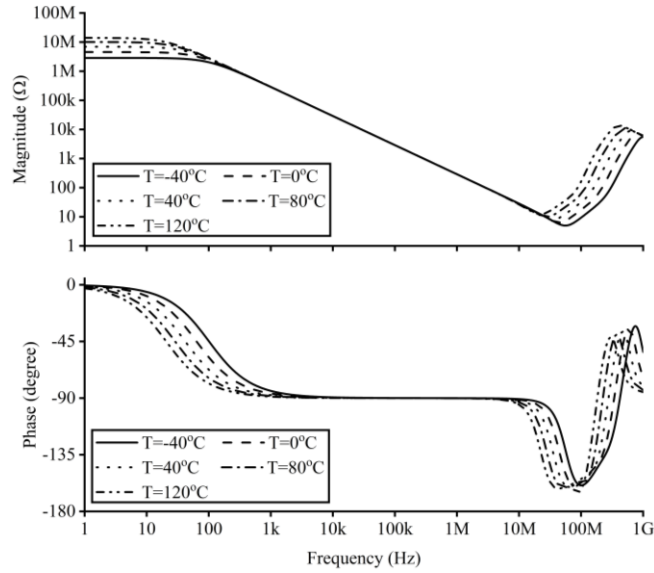
Figure 8. Temperature analysis outcomes of the first proposed FCM
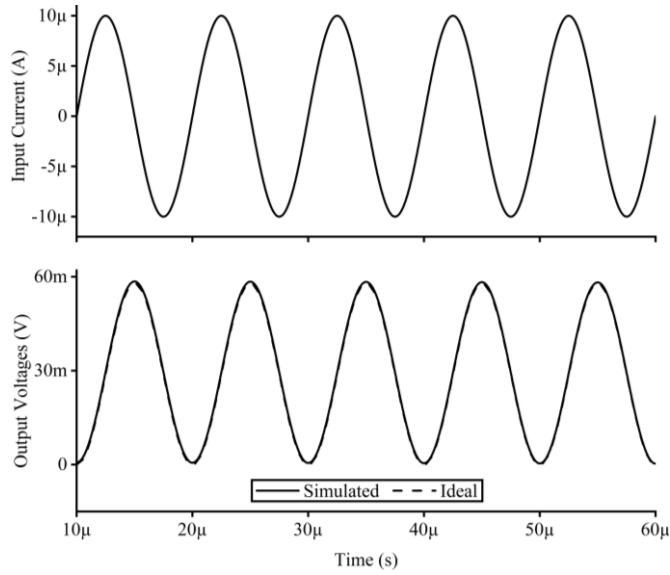
Figure 9. Time-domain analysis outcomes of the first proposed FCM
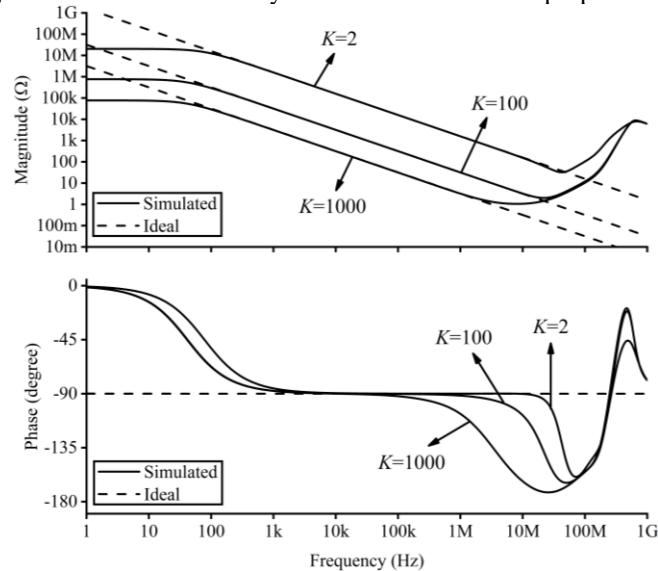
Figure 10. AC analysis outcomes for different *K* values of the first proposed FCM

The first designed FCM is compared with the FCM in (Mohan, 2005). $R_1 = 1$ kΩ, $R_2 = 11$ kΩ, and $C = 50$ pF are chosen for the FCM in (Mohan, 2005). Thus, $K = 11$, and $C_{eq} = 0.55$ nF are obtained. For the first proposed FCM, $R_1 = 10$ kΩ, $R_2 = 1$ kΩ, and $C_1 = 50$ pF are taken; hence, $K = 11$, and $C_{eq} = 0.55$ nF are gotten. The comparison results for the AC simulations are given in **Figure 11**.
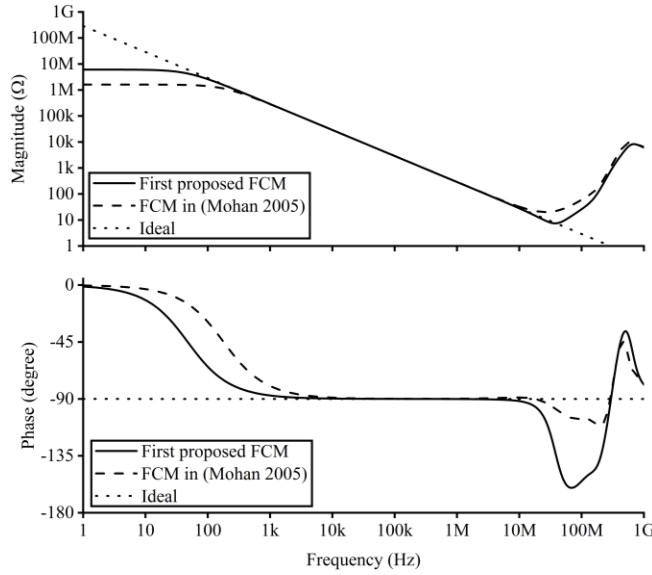
Figure 11. AC analysis outcomes for the FCM in (Mohan, 2005) and the first proposed FCM

4.2. Simulation Results of The Second Proposed FCM

In numerous simulations, C_1, R_1, and R_2 of the second proposed FCM, shown in **Figure 4**, are selected as 50 pF, 10 kΩ, and 1 kΩ, respectively. With these values, K is calculated as 11; consequently, C_{eq} is obtained as 0.55 nF. The second proposed FCM is consumed 1.16 mW of power. Frequency-domain results of the second designed FCM are shown in **Figure 12** comparatively with the theoretical results. Moreover, the MC analysis results of the second proposed FCM are given in **Figure 13**. MC analysis is fulfilled while the uniform deviations of all passive elements are selected as 10%, which is maintained for 150 samples. The temperature analysis results are plotted in **Figure 14**, where the temperature varies from –40°C to 120°C. Additionally, the time-domain analyses of the second proposed FCM are performed. Similarly, the same input currents are applied as in Section 4.1. The input current and output voltages are demonstrated in **Figure 15**. In **Figure 16**, the AC frequency results of the second proposed FCM with different K values are represented. In this analysis, C_1 and R_2 are respectively selected as 50 pF and 1 kΩ. As well, R_1 is separately selected as 1 kΩ, 99 kΩ, and 999 kΩ. As a result, C_{eq} is obtained as 100 pF, 0.5 nF, and 5 nF, while K is evaluated as 2, 100, and 1000, respectively.

Likewise, the second designed FCM is compared with FCM in (Mohan, 2005). The same passive elements given in Section 4.1 are taken. The simulation result is given in **Figure 17** comparatively with the second proposed FCM.
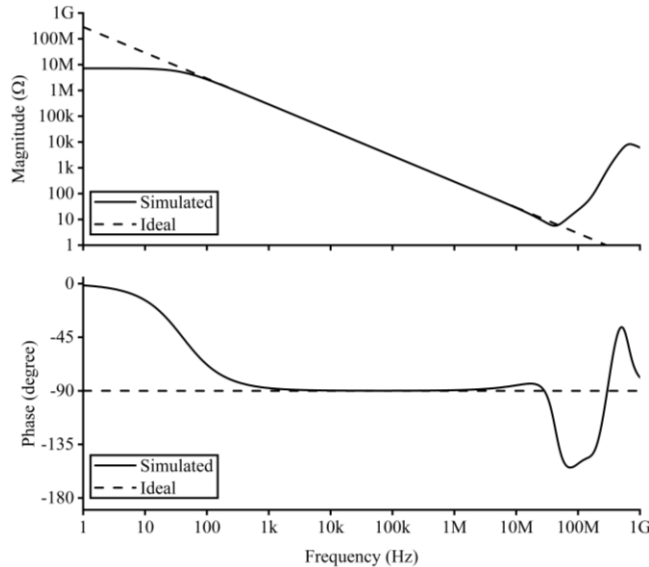
Figure 12. Frequency-domain analysis outcomes of the second proposed FCM
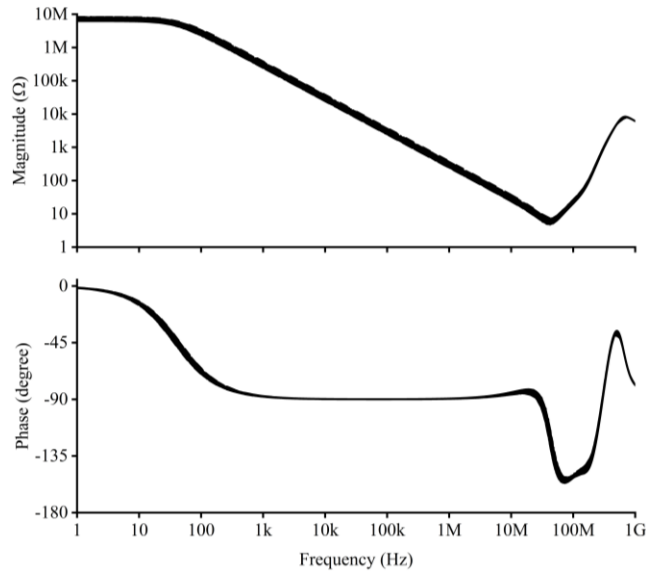
Figure 13. MC analysis outcomes of the second proposed FCM
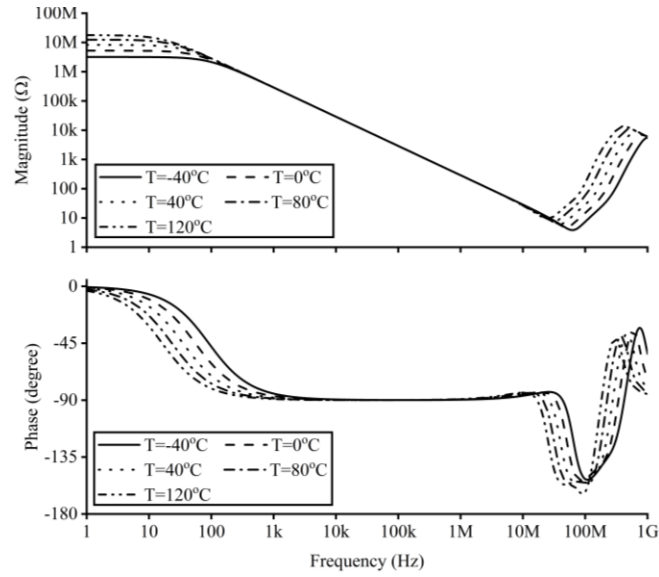
Figure 14. Temperature analysis outcomes of the second proposed FCM
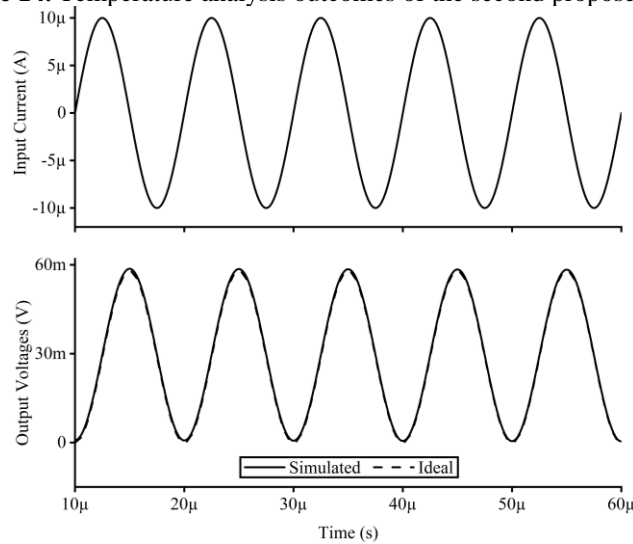
Figure 15. Time-domain analysis outcomes of the second proposed FCM
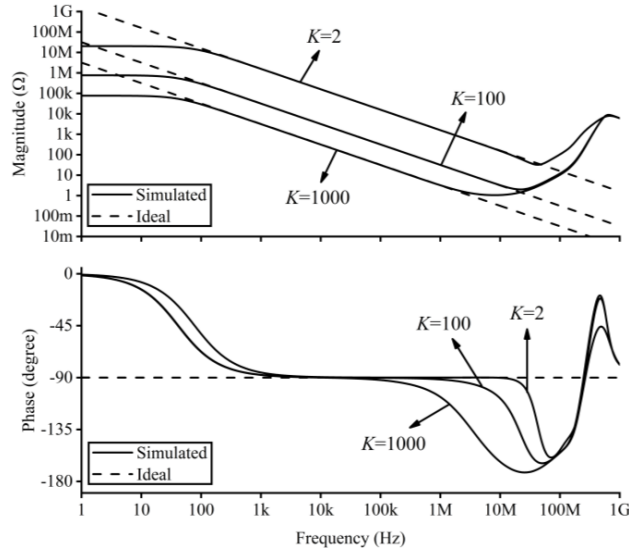
Figure 16. AC analysis outcomes for different *K* values of the second proposed FCM
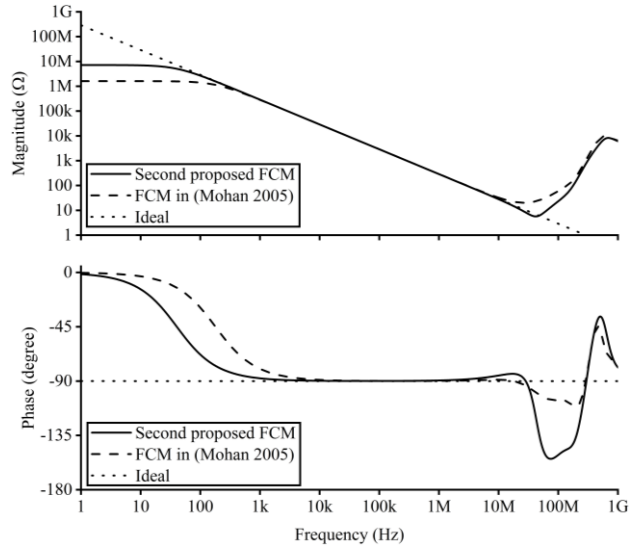
Figure 17. AC analysis outcomes for the second proposed FCM and FCM in (Mohan, 2005)

5. Application Example: Second-order Passive Filter

The proposed FCMs are tested in the second-order passive filter which is represented in **Figure 18**. It can appear from the application example in **Figure 18** that the filter can behave as high-pass (HP) filter or notch filter. The transfer functions of the filter are indicated in equations (9) and (10) for HP and notch outputs, respectively. Also, the resonance frequency (f_0) of the filter is indicated in equation (11), while the quality factor (Q) is in equation (12).
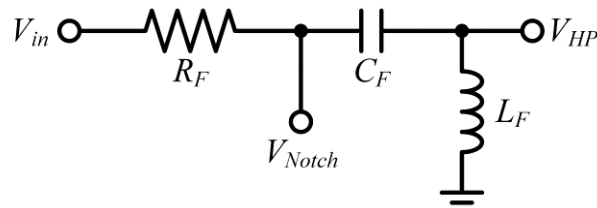
Figure 18. The second-order passive filter

$$\frac{V_{HP}}{V_{in}} = \frac{s^2}{s^2 + s\dfrac{R_F}{L_F} + \dfrac{1}{C_F L_F}} \tag{9}$$

$$\frac{V_{Notch}}{V_{in}} = \frac{s^2 + \dfrac{1}{C_F L_F}}{s^2 + s\dfrac{R_F}{L_F} + \dfrac{1}{C_F L_F}} \qquad (10)$$

$$f_0 = \frac{1}{2\pi\sqrt{C_F L_F}} \qquad (11)$$

$$Q = \frac{1}{R_F}\sqrt{\frac{L_F}{C_F}} \qquad (12)$$

For the simulations, the first proposed FCM is used instead of the C_F in **Figure 18**, firstly. R_F and L_F of the filter are selected as 1 kΩ and 0.5 mH. Also, C_1, R_1, and R_2 in **Figure 3** are respectively chosen as 50 pF, 9 kΩ, and 1 kΩ. Consequently, C_{eq} is ideally evaluated as 0.5 nF, while K is 10. Thus, selecting these values, f_0 of the filter is obtained as about 318 kHz, while Q is 1. Frequency-domain analysis results of the filter are demonstrated in **Figure 19**, and the time-domain analysis results are given in **Figure 20**. In the time-domain analysis, the sinusoidal input voltage is applied with 80 mV peak-to-peak at 1 MHz for the HP output. In addition, the second proposed FCM is utilized instead of C_F in the filter application, while C_1, R_1, and R_2 of the second proposed FCM are selected as 50 pF, 9 kΩ, and 1 kΩ. Also, R_F and L_F of the filter are taken as the same values. Hereby, f_0 and Q of the filter are also obtained as the same values. AC responses and transient analysis results of the filter are demonstrated in **Figure 21** and **Figure 22**, respectively.
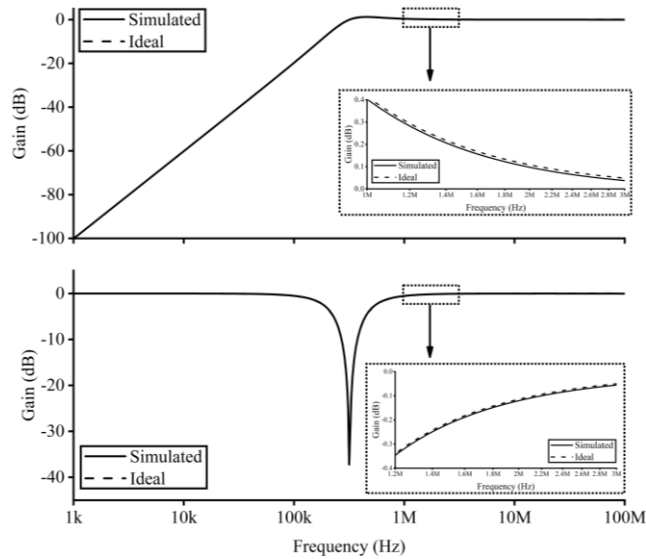
Figure 19. AC analysis outcomes of the filter in which the first proposed FCM used
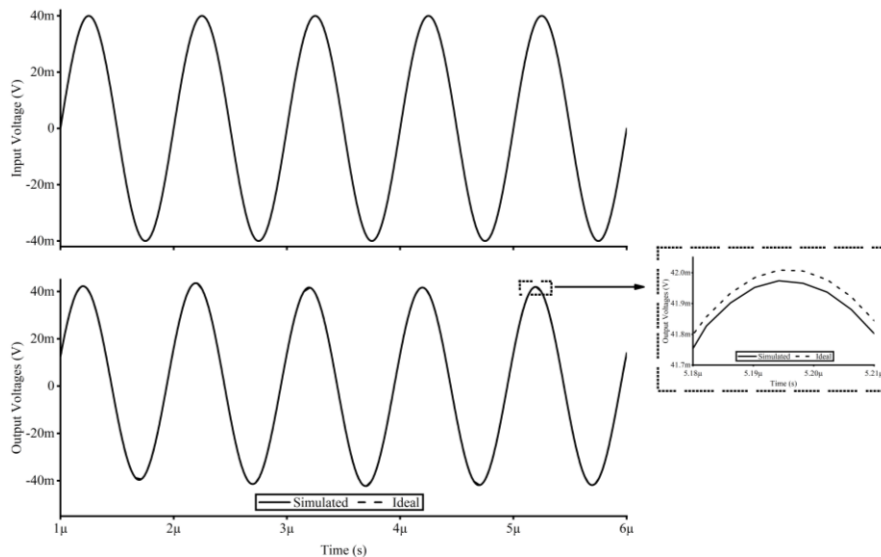
Figure 20. Time-domain analysis outcomes of the filter in which the first proposed FCM used
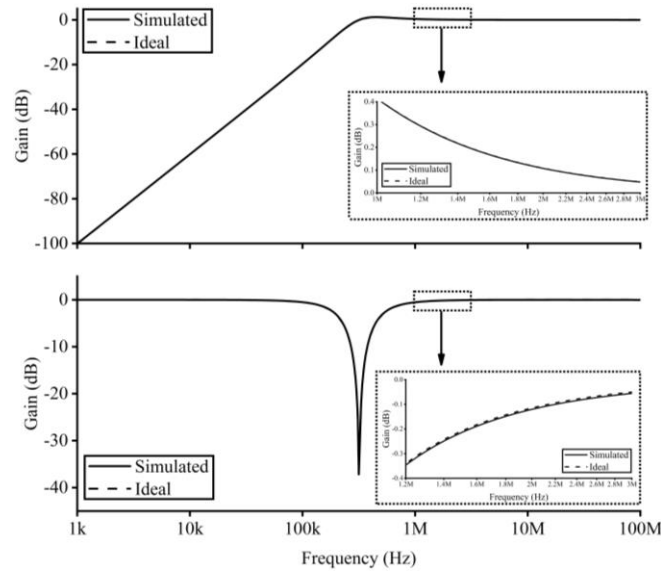
Figure 21. AC analysis outcomes of the filter in which the second proposed FCM used
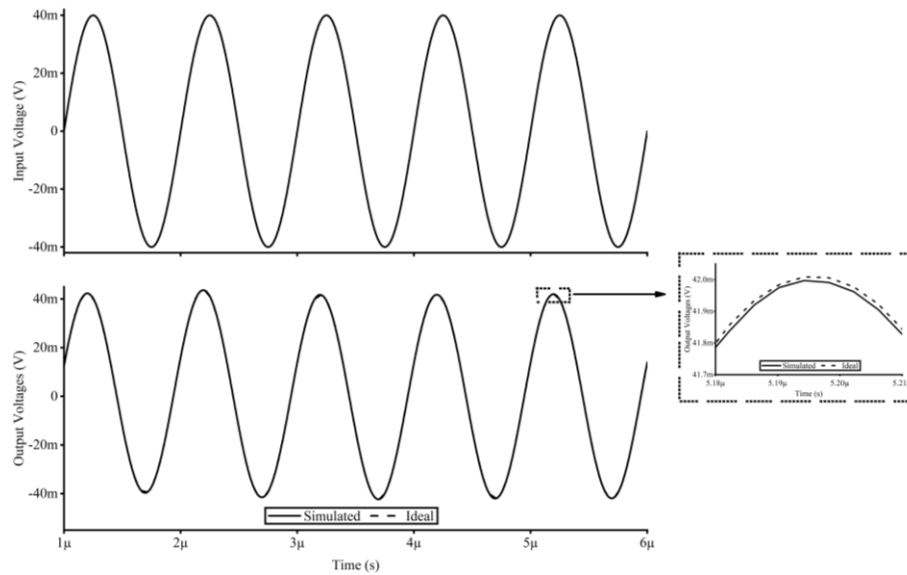
Figure 22. Time-domain analysis outcomes of the filter in which the second proposed FCM used

6. Conclusions

In this paper, two new lossless FCMs are proposed. Only two active devices are used, called DO-CCII, in the proposed FCMs. Both lossless FCMs are designed with a minimum number of passive elements. Resistors of the proposed FCMs are grounded, but a capacitor is floating in both proposed FCMs. The simulation responses of the proposed FCMs are achieved by using the SPICE simulations. Simulation results confirm the theoretical analysis from approximately 100 Hz to 40 MHz. Also, K can be very high. In addition, the proposed FCMs can be electronically adjusted if the current controlled DO-CCIIs are used instead of the DO-CCIIs of the proposed circuits. Both proposed FCMs are applied in the second-order passive filter as an application example. This application example has two outputs, one is HP output, and the other is notch output. Simulations of the filters, in which both proposed FCMs separately used, are verified the ideal results. The SPICE program is used for all the simulations, while 0.18 μm CMOS technology parameters are utilized in the internal structure of the DO-CCIIs.

References

Abuelma'Atti, M. T., & Tasadduq, N. A. (1999). Electronically tunable capacitance multiplier and frequency-dependent negative-resistance simulator using the current-controlled current conveyor. *Microelectronics Journal*, *30*(9), 869–873.

Al-Absi, M. A., & Al-Khulaifi, A. A. (2019). A new floating and tunable capacitance multiplier with large multiplication factor. *IEEE Access*, *7*, 120076–120081.

Amico, A. D., Natale, C. Di, Mariucci, M., & Barccarani, G. (1997). Active capacitance multiplication for sensor application. *Proceedings of Italian Conference of Sensors and Microsystems*.

Ferri, G., & Guerrini, N. C. (2001). Low-voltage low-power novel CCII topologies and applications. *ICECS 2001. 8th IEEE International Conference on Electronics, Circuits and Systems*, 1095–1098.

Giuseppe, F., & Guerrini, N. C. (2004). *Low-voltage low-power CMOS current conveyors*. Kluwer Academic Publishers.

Hassanein, W. S., Awad, I. A., & Soliman, A. M. (2005). New high accuracy CMOS current conveyors. *AEU - International Journal of Electronics and Communications*, *59*(7), 384–391.

Jaikla, W., & Siripruchyanun, M. (2007). Realization of current conveyors-based floating simulator employing grounded passive elements. *Proc. ECTI Con*, 89–92.

Kuntman, H. H., & Uygur, A. (2012). New possibilities and trends in circuit design for analog signal processing. *2012 International Conference on Applied Electronics*, 1–9.

Minaei, S., & Yuce, E. (2010). Novel voltage-mode all-pass filter based on using DVCCs. *Circuits, Systems, and Signal Processing*, *29*, 391–402.

Minaei, S., Yuce, E., & Cicekoglu, O. (2006). A versatile active circuit for realising floating inductance, capacitance, FDNR and admittance converter. *Analog Integrated Circuits and Signal Processing*, *47*(2), 199–202.

Mohan, P. V. A. (2005). Floating capacitance simulation using current conveyors. *Journal of Circuits, Systems, and Computers*, *14*(1), 123–128.

Pal, K. (1981). New inductance and capacitor floatation schemes using current conveyors. *Electronics Letters*, *17*(21), 807–808.

Petchakit, W., & Petchakit, S. (2005). New floating capacitance multipliers. *Proceedings of 28th Electrical Engineering Conference (EECON-28)*, *2*, 1233–1236.

Saad, R. A., & Soliman, A. M. (2010). On the systematic synthesis of CCII-based floating simulators. *International Journal of Circuit Theory and Applications*, *38*(9), 935–967.

Sagbas, M., Ayten, U. E., Sedef, H., & Koksal, M. (2009). Floating immittance function simulator and its applications. *Circuits, Systems, and Signal Processing*, *28*(1), 55–63.

Senani, R. (1982). Novel lossless synthetic floating inductor employing a grounded capacitor. *Electronics Letters*, *18*(10), 413–414.

Senani, R., Bhaskar, D. R., & Singh, A. K. (2015). *Current conveyors: variants, applications and hardware implementations*. Springer International Publishing.

Siripruchyanun, M., Phattanasak, M., & Jaikla, W. (2007). Temperature-insensitive, current conveyor-based floating simulator topology. *2007 International Symposium on Integrated Circuits*, 65–68.

Toumazou, C., Lidgey, F. J., & Haigh, D. G. (1993). *Analogue IC design: the current-mode approach*. The Institution of Engineering and Technology.

Wilson, B. (1990). Recent developments in current conveyors and current-mode circuits. *IEE Proceedings G (Circuits, Devices and Systems)*, *137*(2), 63–77.

Wilson, B. (1992). Tutorial review trends in current conveyor and current-mode amplifier design. *International Journal of Electronics*, *73*(3), 573–583.

Yuce, E. (2006a). Floating inductance, FDNR and capacitance simulation circuit employing only grounded passive elements. *International Journal of Electronics*, *93*(10), 679–688.

Yuce, E. (2006b). On the realization of the floating simulators using only grounded passive components. *Analog Integrated Circuits and Signal Processing*, *49*(2), 161–166.

Yuce, E. (2017). DO-CCII/DO-DVCC based electronically fine tunable quadrature oscillators. *Journal of Circuits, Systems and Computers*, *26*(2), 1–17.

Yuce, E., Cicekoglu, O., & Minaei, S. (2006). CCII-based grounded to floating immittance converter and a floating inductance simulator. *Analog Integrated Circuits and Signal Processing*, *46*(3), 287–291.

Yuce, E., Minaei, S., & Cicekoglu, O. (2006). Resistorless floating immittance function simulators employing current controlled conveyors and a grounded capacitor. *Electrical Engineering*, *88*(6), 519–525.

Yucehan, T., & Yuce, E. (2022). CCII-based simulated floating inductor and floating capacitance multiplier. *Analog Integrated Circuits and Signal Processing*, *112*, 417–432.